



# HHS Public Access

## Author manuscript

*J Chem Health Saf.* Author manuscript; available in PMC 2022 September 21.

Published in final edited form as:

*J Chem Health Saf.* 2021 July 26; 28(4): 268–278. doi:10.1021/acs.chas.0c00129.

## Large-Format Additive Manufacturing and Machining Using High-Melt-Temperature Polymers. Part II: Characterization of Particles and Gases

**Aleksandr B. Stefaniak,**

National Institute for Occupational Safety and Health, Morgantown, West Virginia 26505, United States

**Lauren N. Bowers,**

National Institute for Occupational Safety and Health, Morgantown, West Virginia 26505, United States

**Stephen B. Martin Jr.,**

National Institute for Occupational Safety and Health, Morgantown, West Virginia 26505, United States

**Duane R. Hammond,**

National Institute for Occupational Safety and Health, Cincinnati, Ohio 45213, United States

**Jason E. Ham,**

National Institute for Occupational Safety and Health, Morgantown, West Virginia 26505, United States

**J. R. Wells,**

National Institute for Occupational Safety and Health, Morgantown, West Virginia 26505, United States

**Alyson R. Fortner,**

National Institute for Occupational Safety and Health, Morgantown, West Virginia 26505, United States

**Alycia K. Knepp,**

National Institute for Occupational Safety and Health, Morgantown, West Virginia 26505, United States

**Sonette du Preez,**

North-West University, Occupational Hygiene and Health Research Initiative, Potchefstroom 2520, South Africa

---

**Corresponding Author** Phone: +1-304-285-6302; AStefaniak@cdc.gov.

Complete contact information is available at: <https://pubs.acs.org/10.1021/acs.chas.0c00129>

**Supporting Information**

The Supporting Information is available free of charge at <https://pubs.acs.org/doi/10.1021/acs.chas.0c00129>.

Details of the carbonyl and BPA/BPS analyses, number and type of samplers by polymer and print job, an SEM image of diffuse cluster particles, tabulated data for all analytes by polymer and print job, and analytical limits of detection for each substance (PDF)

The authors declare no competing financial interest.

**Jack R. Pretty,**

National Institute for Occupational Safety and Health, Cincinnati, Ohio 45213, United States

**Jennifer L. Roberts,**

National Institute for Occupational Safety and Health, Cincinnati, Ohio 45213, United States

**Johan L. du Plessis,**

North-West University, Occupational Hygiene and Health Research Initiative, Potchefstroom 2520, South Africa

**Austin Schmidt,**

Additive Engineering Solutions, Akron, Ohio 44305, United States

**Matthew G. Duling,**

National Institute for Occupational Safety and Health, Morgantown, West Virginia 26505, United States

**Andrew Bader,**

Additive Engineering Solutions, Akron, Ohio 44305, United States

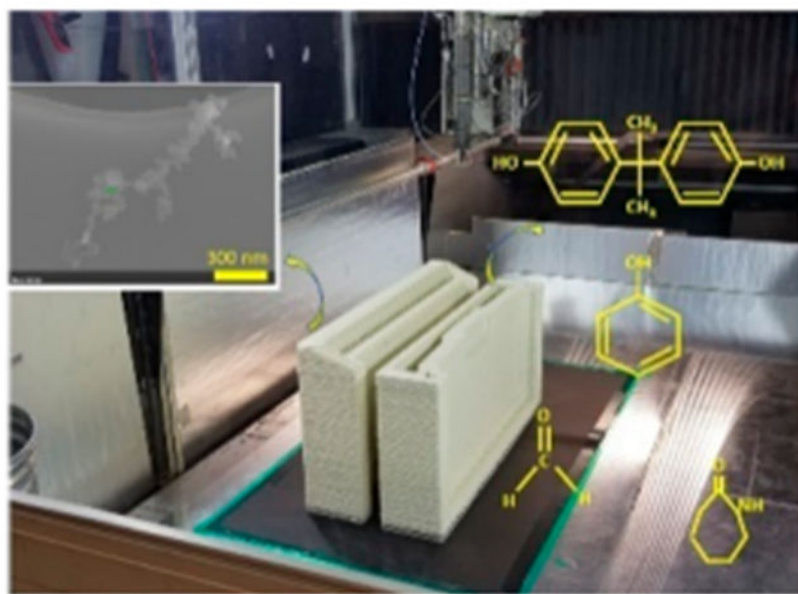
**M. Abbas Virji**

National Institute for Occupational Safety and Health, Morgantown, West Virginia 26505, United States

**Abstract**

Extrusion of high-melt-temperature polymers on large-format additive manufacturing (LFAM) machines releases particles and gases, though there is no data describing their physical and chemical characteristics. Emissions from two LFAM machines were monitored during extrusion of acrylonitrile butadiene styrene (ABS) and polycarbonate (PC) polymers as well as high-melt-temperature Ultem (poly(ether imide)), polysulfone (PSU), poly(ether sulfone) (PESU), and polyphenylene sulfide (PPS) polymers. Filter samples of particles were collected for quantification of elements and bisphenol A and S (BPA, BPS) and visualization of morphology. Individual gases were quantified on substance-specific media. Aerosol sampling demonstrated that concentrations of elements were generally low for all polymers, with a maximum of 1.6 mg/m<sup>3</sup> for iron during extrusion of Ultem. BPA, an endocrine disruptor, was released into air during extrusion of PC (range: 0.4 ± 0.1 to 21.3 ± 5.3 µg/m<sup>3</sup>). BPA and BPS (also an endocrine disruptor) were released into air during extrusion of PESU (BPA, 2.0–8.7 µg/m<sup>3</sup>; BPS, 0.03–0.07 µg/m<sup>3</sup>). Work surfaces and printed parts were contaminated with BPA (<8–587 ng/100 cm<sup>2</sup>) and BPS (<0.22–2.5 ng/100 cm<sup>2</sup>). Gas-phase sampling quantified low levels of respiratory irritants (phenol, SO<sub>2</sub>, toluene, xylenes), possible or known asthmagens (caprolactam, methyl methacrylate, 4-oxopentanal, styrene), and possible occupational carcinogens (benzene, formaldehyde, acetaldehyde) in air. Characteristics of particles and gases released by high-melt-temperature polymers during LFAM varied, which indicated the need for polymer-specific exposure and risk assessments. The presence of BPA and BPS on surfaces revealed a previously unrecognized source of dermal exposure for additive manufacturing workers using PC and PESU polymers.

**Graphical Abstract**



### Keywords

additive manufacturing; 3-D printing; irritants; asthmagens; carcinogens; bisphenols

## INTRODUCTION

Large-format additive manufacturing (LFAM) machines operate on the principle of material extrusion. In our Part I companion paper, which focused on real-time monitoring to determine emission rates, it was reported that LFAM extrusion of acrylonitrile butadiene styrene (ABS) and polycarbonate (PC) as well as high-melt-temperature polymers such as Ultem (poly(ether imide)), polysulfone (PSU), polyphenylene sulfide (PPS), and poly(ether sulfone) (PESU) emitted particles and gases.<sup>1</sup> Some investigators have characterized the chemical and physical properties of emissions from material extrusion of ABS, PC, and Ultem polymers, usually generated by desktop-scale 3-dimensional fused filament fabrication (FFF) “3-D” printers and, less frequently, from larger industrial-scale FFF machines.<sup>2–20</sup> These studies indicated that the chemical composition of particles and gases released during extrusion, and their levels, differed among polymers. To our knowledge, there are no data on the composition of particles and gases released during LFAM, particularly during extrusion of high-melt-temperature polymers.

For ABS, the chemistry of particles and gases released during additive manufacturing is an important factor in adverse toxicological and human health effects.<sup>21–25</sup> It is reasonable that the chemistry of particles and gases released from other types of polymers used in material extrusion additive manufacturing may include substances that negatively impact human health. Herein, we report the characteristics of particles and gases released during LFAM with six different polymers that span a range of melt temperatures.

## MATERIALS AND METHODS

Details of the facility, including the floor plan, LFAM machines, and room ventilation characteristics, were provided in the Part I companion paper.<sup>1</sup> Briefly, all measurements were collected in a 3000 m<sup>3</sup> room with two LFAM machines (LFAM-1, 76 m<sup>3</sup> internal volume; LFAM-2, 50 m<sup>3</sup> internal volume). Both machines have solid metal and clear plastic sidewalls with nonsealing doors at the front and back. LFAM-1 had a custom-built loose-fitting canopy made of plastic tarpaulin fitted over a frame to enclose the build volume. LFAM-2 had a custom-built loose-fitting canopy made of reflective bubble roll insulation fitted over a frame to enclose the build volume. Table 1 summarizes the extrusion conditions for ABS, PC, Ultem, PPS, PSU, and PESU polymers printed on these machines. All polymer pellets contained carbon fiber (CF) and/or glass fiber (GF) additive to provide structural support for large builds. All polymers were black in color, except for ABS with GF additive, which was white.

### Air Monitoring for Particles.

Airborne particles were collected onto 5.0 or 3.0  $\mu\text{m}$  pore size track-etched polycarbonate filters (TEPC, SKC Inc., Eighty Four, PA) mounted in open-face 37 mm cassettes by drawing air through the membrane at 4.0 L/min using calibrated sampling pumps (AirChek XR5000, SKC Inc.). Filters were analyzed off-line using a field emission-scanning electron microscope (FE-SEM, S-4800, Hitachi, Tokyo, Japan) to evaluate morphology and size and energy-dispersive X-ray (EDX) analysis (Quantax, Bruker Scientific Instruments, Berlin, Germany) to identify elemental constituents. Separate samples of airborne particles were collected onto 0.8  $\mu\text{m}$  pore size mixed cellulose ester filters (MCE, product no. 225-3-01, SKC Inc.) mounted in closed-face cassettes by drawing air through the membrane at 3.0 L/min using calibrated sampling pumps (AirChek XR5000, SKC Inc.). These filters were analyzed off-line to quantify elements by inductively coupled plasma-optical emission spectrometry (ICP-OES) in accordance with National Institute for Occupational Safety and Health (NIOSH) Method 7303.

### Air Monitoring for Individual Volatile Organic Compound Gases.

Volatile organic compound (VOC) gases were collected using 450 mL Silonite-coated evacuated canister samples (Model 29-MC450SQT, Entech Instruments Inc., Simi Valley, CA) with flow-controllers (preset to sample for a specific time duration, e.g., 4, 8, or 12 h) followed by quantification of 15 specific compounds by off-line analysis using gas chromatography-mass spectrometry (GC-MS) in accordance with NIOSH Method 3900.

### Possible Breakdown Products of Specific Polymers.

As summarized in Table 1, several substances may be released in the form of particles or gases that are unique to the thermal breakdown of a specific polymer. Samples for airborne particulate bisphenol A (BPA) and bisphenol S (BPS) were collected by drawing workplace air through 1.0  $\mu\text{m}$  pore-size 37 mm glass fiber filters (GFFs, product no. 225-709, SKC Inc.) or 25 mm quartz fiber filters (QFFs, product no. 225-401-25, SKC Inc.) mounted in closed-face cassettes at 0.2 L/min using calibrated sampling pumps (Pocket Pump TOUCH, SKC Inc.). After collection, samples were extracted with acetonitrile and water and analyzed

using liquid chromatography–mass spectrometry (LC–MS) as detailed in the Supporting Information.

Sampling for gas-phase aldehyde compounds was initially performed by using a calibrated sampling pump at 4.0 L/min to draw air into 25 mL of deionized water in a 60 mL Teflon bubbler (Savillex, Eden Prairie, MN). After collection, samples were derivatized and analyzed using GC–MS (details in the Supporting Information).<sup>38–40</sup> On later surveys, air samples for aldehydes were collected using a cartridge that contained silica gel coated with 2,4-dinitrophenylhydrazine (DNPH) (product no. 226-119, SKC Inc.) at 0.2–0.4 L/min using calibrated sampling pumps (Pocket Pump TOUCH, SKC Inc.) and analyzed by high-performance liquid chromatography with ultraviolet detection (HPLC-UV) in accordance with NIOSH Method 2016.

Samples for airborne caprolactam were collected using Occupational Safety and Health Administration (OSHA) versatile sampler (OVS-7) tubes that contained a glass fiber filter and two sections of XAD-7 adsorbent (product no. 226-57, SKC Inc.) at 0.1–0.4 L/min (depending on print duration) using calibrated personal sampling pumps (Pocket Pump TOUCH, SKC Inc.) and analyzed by HPLC-UV in accordance with OSHA Method PV2012. Chlorobenzene was sampled on coconut shell charcoal tubes (product no. 226-01, SKC Inc.) at 0.125 L/min using calibrated sampling pumps (Pocket Pump TOUCH, SKC Inc.) and measured using GC with a flame ionization detector (GC-FID) in accordance with NIOSH Method 1003. Phenol was collected on XAD-7 sorbent tubes (product no. 226-95, SKC Inc.) at 0.125 L/min using calibrated sampling pumps (Pocket Pump TOUCH, SKC Inc.) and analyzed using GC-FID in accordance with NIOSH Method 2546. Particulate sulfate  $\text{SO}_4^{2-}$  and gaseous sulfur dioxide ( $\text{SO}_2$ ) were collected using a sampler that consisted of a 0.8  $\mu\text{m}$  pore-size 37 mm cellulose ester filter followed by a sodium carbonate-treated cellulose ester filter in a cassette (product no. 225-9005, SKC Inc.) at 1.0–2.0 L/min using calibrated sampling pumps (AirChek XR5000, SKC Inc.). Samples were analyzed using ion chromatography in accordance with NIOSH Method 6004. Hydrogen sulfide ( $\text{H}_2\text{S}$ ) gas was sampled using a sorbent tube that contained silica gel coated with silver nitrate and a glass fiber filter treated with sodium carbonate/glycerol silver nitrate (product no. 226-177, SKC Inc.) at 0.2 L/min using calibrated sampling pumps (Pocket Pump TOUCH, SKC Inc.). Samples were analyzed by ion chromatography using a conductivity detector in accordance with OSHA Method 1008. The number and types of time-integrated samples collected for each polymer by print job are summarized in the Supporting Information. Temperature and relative humidity were recorded during sampling using a real-time monitor (IAQ-Calc, Model 7545, TSI Inc., Shoreview, MN). Separate time-integrated samples were collected prior to the start of a task (background) and during the task (printing), and all results presented are background-corrected values.

### Placement of Air Monitoring Equipment.

Sampling was performed by placing a time-integrated TEPC filter, MCE filter, and canister sampler in a wire metal basket that was positioned outside or inside an LFAM enclosure. Depending on the polymer, time-integrated BPA/BPS, aldehyde, caprolactam, phenol, chlorobenzene,  $\text{H}_2\text{S}$ , and  $\text{SO}_4^{2-}/\text{SO}_2$  samplers were included as appropriate. The floor plan

of the printer room and the locations of sampling baskets is shown in the companion article.<sup>1</sup> At LFAM-1, the inside basket was placed at the front of the machine enclosure, and the outside basket was placed at the platform that the operator normally occupied during work. At LFAM-2, the inside basket was placed on the floor at the front of the machine enclosure in a location that did not interfere with the moving extruder nozzle, and the outside basket was placed at the computer control station that the operator normally occupied during work. Baskets located inside of the enclosures were positioned with the sampler inlets approximately 0.3–0.5 m above the floor, and baskets located outside of the enclosures at the operator locations were positioned with the sampler inlets at breathing zone height. Depending on the size and shape of the print, duration of polymer extrusion, and positioning of the print on the print bed (front, back, etc.), additional pairs of canister and TEPC and MCE filters were positioned inside and outside of the enclosure on a side and/or the rear of the machine. All samplers for each polymer/print job combination were turned on at the same time at the start of printing and turned off at the same time at the end of printing.

For ABS, a total of seven separate print jobs were monitored (designated as ABS-1 to ABS-7). Note that, in the Part I companion article, only six ABS print jobs were reported because, for job ABS-7, only time-integrated samples were collected. ABS-4 and ABS-5 were short-duration print jobs that were performed sequentially, which necessitated collection of composite time-integrated samples to increase the masses of material for analysis (i.e., the same samplers were used for jobs ABS-4 and ABS-5 combined). For PC polymer, a total of four separate print jobs were monitored (designated as PC-1–PC-4). For PPS polymer, four sequential print jobs were attempted throughout 1 day. The first two PPS polymer print attempts failed because of nozzle clogging. (As described in the Part I paper, the real-time particle concentration profile consisted of a single large peak, so these attempts were grouped as job PPS-1.) The latter two PPS polymer print jobs were successful (designated as PPS-2 and PPS-3). Given the short duration of these print jobs, composite air samples were collected for jobs PPS-1–PPS-3 to increase the masses of analyte on media. For Ultem, PSU, and PESU, a total of two print jobs were monitored for each polymer type (designated Ultem-1, Ultem-2, PSU-1, etc.). During our initial site visit (print jobs ABS-1, Ultem-1, and Ultem-2), a basket was only placed outside a machine enclosure at the operator's workstation. Thereafter, one basket was positioned inside an LFAM machine enclosure, and one basket was positioned outside of its enclosure.

### Surface Wipe Sampling.

To evaluate whether potential exists for skin exposure to BPA or BPS from contact with surfaces during work with these PC and PESU polymers, wipe samples were collected from various surfaces. In the 3000 m<sup>3</sup> print room, wipe samples were collected from the LFAM-1 machine (computer, door handles, and walls). Adjacent to the print room, the facility housed a separate machining bay with several milling and cutting machines. In the machining bay, wipe samples were collected from office equipment, two milling machines used for postprint processing of parts, acrylic panel walls surrounding the milling machines, and printed objects. The facility was built new, so there was no history of prior BPA or BPS use at this site that could bias results; however, surface wipe sampling was not done at the time the facility opened to establish baseline levels. Surface wipe samples were

collected by wetting a swab (Alpha Swabs, part no. TX715, Texwipe, Kernersville, NC) with HPLC-grade isopropyl alcohol that was lightly rubbed across a surface demarcated using a disposable 10 cm × 10 cm cardboard template (part no. 225-2415A, SKC Inc.) in a regular pattern (top to bottom, left to right, 45° angle) to ensure that a constant area was sampled each time.<sup>41</sup> After collection, samples were extracted with acetonitrile and water and analyzed using LC–MS (see the Supporting Information).

## Data Analysis.

Data plots were prepared using SigmaPlot (version 14.0, Systat Software, Inc., San Jose, CA). For all box plots, the bottom whisker is the 10th percentile, the bottom of the box the 25th percentile, the line within the box the median, the top boundary of the box the 75th percentile, and the top whisker the 90th percentile. Solid circles are outlier values. Descriptive statistics (mean, standard deviation) were computed in JMP (version 13, SAS Institute Inc., Cary, NC).

## RESULTS

Characteristics of particles and gases are summarized herein by polymer type. In general, characteristics varied by polymer and included substances of health concern.

## Acrylonitrile Butadiene Styrene.

Inspection of TEPC filters by SEM-EDX revealed nanoscale particles with a cluster morphology composed of carbon and oxygen. These cluster particles were observed in filter samples collected during extrusion of all polymers (see Figure S1). Long micron-scale fibers that were composed of aluminum and silicon were observed on some TEPC filter samples from printing with ABS polymer that contained GF additive (Figures 1a and 2a). Fibers composed of carbon and oxygen were present on filter samples from printing with ABS polymer that contained CF additive (images and spectra not shown). Nine elements were quantified on MCE filter samples collected during print jobs ABS-1–ABS-3 and ABS-7 (samples were not collected for print jobs ABS-4–ABS-6); the highest measured concentration was iron at  $558 \mu\text{g}/\text{m}^3$  (see Table S1).

Figure 3a summarizes the time-integrated sampling results for select VOCs quantified during extrusion of ABS (results by print job are given in Table S1). Ten different VOCs were quantified using canister samplers: acetaldehyde (7.0–34.6  $\mu\text{g}/\text{m}^3$ ), acetone (2.2–263.6  $\mu\text{g}/\text{m}^3$ ), benzene (1.2–50.6  $\mu\text{g}/\text{m}^3$ ), d-limonene (8.9–31.3  $\mu\text{g}/\text{m}^3$ ), methyl methacrylate (0.3–43.2  $\mu\text{g}/\text{m}^3$ ),  $\alpha$ -pinene (5.1  $\mu\text{g}/\text{m}^3$ ), styrene (8.5–170.9  $\mu\text{g}/\text{m}^3$ ), toluene (2.3–201.3  $\mu\text{g}/\text{m}^3$ ), *m,p*-xylene (1.7–43.9  $\mu\text{g}/\text{m}^3$ ), and *o*-xylene (36.8  $\mu\text{g}/\text{m}^3$ ); not all substances were detected for all print jobs. Carbonyl compounds detected using impinger and DNPH cartridge samplers included benzaldehyde (0.8  $\mu\text{g}/\text{m}^3$ ), formaldehyde (0.4–12.8  $\mu\text{g}/\text{m}^3$ ), and 4-oxopentanal (0.8  $\mu\text{g}/\text{m}^3$ ). Caprolactam was detected on one sample collected inside an LFAM machine enclosure (22.0  $\mu\text{g}/\text{m}^3$ ).

### Polycarbonate.

Aerosol particles released during extrusion of PC included spherical-shaped micron-scale particles composed of carbon and oxygen (not shown) and fiber fragments of respirable size that were composed of carbon and oxygen, consistent with CF additive (see Figures 1b and 2b). Fibers were identified on filter samples collected inside and outside of the LFAM machine enclosures. Trace concentrations (no greater than  $0.8 \mu\text{g}/\text{m}^3$ ) of aluminum, antimony, barium, copper, iron, manganese, nickel, tin, titanium, and zinc were quantified on MCE filter samples (see Table S2).

BPA was not detected on any background samples. During extrusion of PC polymer (job PC-2), the average concentrations of airborne BPA were  $0.4 \pm 0.1 \mu\text{g}/\text{m}^3$  (outside enclosure) and  $4.8 \pm 4.0 \mu\text{g}/\text{m}^3$  (inside enclosure). In the afternoon on the same day, average airborne concentrations of BPA for print job PC-3 were  $1.3 \pm 0.2 \mu\text{g}/\text{m}^3$  (outside enclosure) and  $21.3 \pm 5.3 \mu\text{g}/\text{m}^3$  (inside enclosure). For both print jobs PC-2 and PC-3, BPA concentrations were higher inside and outside of the enclosure at the side and back locations of the LFAM compared with the front where the operator was stationed. BPS was not detected on any background samples or samples collected during extrusion of PC polymer (limit of detection = 0.18 ng/filter).

Results of time-integrated sampling for select VOCs are summarized in Figure 3b. Nine VOCs were quantified in at least one canister sampler. Concentrations for some VOCs of interest were benzene ( $5.4\text{--}18.5 \mu\text{g}/\text{m}^3$ ), ethylbenzene ( $10.1\text{--}34.3 \mu\text{g}/\text{m}^3$ ), styrene ( $15.6\text{--}49.2 \mu\text{g}/\text{m}^3$ ), toluene ( $18.9\text{--}298.6 \mu\text{g}/\text{m}^3$ ), and *m*- and *p*-xylenes ( $9.5\text{--}37.0 \mu\text{g}/\text{m}^3$ ). No single VOC was detected consistently in all canister samples, and only two, acetone and toluene, were detected during all four print jobs. Caprolactam was not detected in air samples. See Table S2 for detailed results by print job.

### Ultem.

Particles collected on TEPC filters at the operator's platform during extrusion of Ultem included micron-scale particles that contained iron (see Figures 1c and 2c); CFs were not observed on any of these samples. Aluminum, arsenic, cadmium, chromium, copper, manganese, and nickel were quantified on MCE filter samples collected during extrusion but did not exceed  $4 \mu\text{g}/\text{m}^3$  (see Table S3). Higher concentrations were detected for zinc (up to  $101 \mu\text{g}/\text{m}^3$ ) and iron (up to  $1600 \mu\text{g}/\text{m}^3$ ).

A box plot of results for select VOCs is given in Figure 3c. Six different VOCs were quantified on canister samples; acetone was present at the highest concentrations ( $74.7\text{--}406.5 \mu\text{g}/\text{m}^3$ ). Impinger sampling detected six different carbonyls, including formaldehyde ( $18.8 \mu\text{g}/\text{m}^3$ ) and 4-oxopentanal ( $1.0\text{--}1.6 \mu\text{g}/\text{m}^3$ ).

### Polyphenylene Sulfide.

Particles collected on TEPC filters during extrusion of PPS included submicron particles that contained sulfur (Figures 1d and 2d) and micron-scale CF (not shown). Analysis of MCE composite filter samples for print jobs PPS-1–PPS-3 yielded quantitative results for only aluminum ( $42.9 \mu\text{g}/\text{m}^3$ ) on one of six samples (see Table S4).

Results of the time-integrated sampling for select VOCs during extrusion of PPS polymer for print jobs PPS-1 to PPS-3 combined are summarized in Figure 3d, and details are given in Table S4. Eight different VOCs were quantified by canister sampling, with acetone present at the highest concentrations (ranging from approximately 300 to 400  $\mu\text{g}/\text{m}^3$ ).  $\text{H}_2\text{S}$  gas was not detected on either sample collected. Sampling media for  $\text{SO}_2$  was unavailable the day that PPS polymer was extruded.

### Polysulfone.

SEM-EDX analysis of airborne particles identified nanoscale compact particles that contained sulfur (Figures 1e and 2e) and micron-scale fibers composed of carbon and oxygen consistent with CF fiber additive (not shown). For print job PSU-1, only traces of titanium and zinc were detected on MCE filter samples. For print job PSU-2, low levels of aluminum (11.9–22.0  $\mu\text{g}/\text{m}^3$ ) and iron (25.0  $\mu\text{g}/\text{m}^3$ ) were quantified on air samples as were traces (no more than 2  $\mu\text{g}/\text{m}^3$ ) of barium, titanium, vanadium, and zinc (Table S5). Sampling media for BPA/BPS was unavailable the day that PSU polymer was extruded.

Results of the time-integrated sampling for select VOCs during extrusion of PSU polymer are summarized in Figure 3e, and detailed results by print job are given in Table S5. Low levels of airborne styrene, *m,p*-xylene, and toluene were measured on samples collected during print job PSU-1 but not during job PSU-2. In contrast, low levels of acetone, benzene, *d*-limonene, and methyl methacrylate were only quantified on print job PSU-2 samples.  $\text{SO}_4^{2-}$  particulate ( $1.5 \pm 0.9 \mu\text{g}/\text{m}^3$ ) and  $\text{SO}_2$  gas ( $20.1 \pm 3.2 \mu\text{g}/\text{m}^3$ ) were only detected on samples collected during print job PSU-2. The observed differences in VOCs and inorganic gases released during printing might be related to the difference in mass of polymer extruded between print jobs PSU-1 (19 kg) and PSU-2 (207 kg).

### Poly(ether sulfone).

SEM-EDX analysis of airborne particles identified nanoscale compact particles that contained calcium (not shown) and micron-scale particles composed of calcium, sulfur, and titanium (see Figures 1f and 2f). Calcium was identified in a majority of particles. MCE filter sampling quantified low levels of aluminum (up to 4.5  $\mu\text{g}/\text{m}^3$ ) and traces ( $<1 \mu\text{g}/\text{m}^3$ ) of barium, cadmium, copper, iron, titanium, and zinc (see Table S6). Airborne BPA levels outside and inside the LFAM enclosure ranged from 2.0 to 8.7  $\mu\text{g}/\text{m}^3$  and from 1.7 to 5.7  $\mu\text{g}/\text{m}^3$ , respectively. Airborne BPS levels ranged from 0.04 to 0.7  $\mu\text{g}/\text{m}^3$  (outside enclosure) and 0.03 to 0.06  $\mu\text{g}/\text{m}^3$  (inside enclosure).

Figure 3f summarizes the time-integrated sampling results for select substances quantified during extrusion of PESU polymer (detailed results by print job are summarized in Table S6). Acetaldehyde (3.8–17.1  $\mu\text{g}/\text{m}^3$ ) and benzene (0.3–1.6  $\mu\text{g}/\text{m}^3$ ) were quantified on all canister samples, and phenol (14.4–25.6  $\mu\text{g}/\text{m}^3$ ) was quantified on all XAD-7 tube samples. Chlorobenzene was not detected on any charcoal tube samples.  $\text{SO}_2$  was quantified on three of four samples (25.0–39.7  $\mu\text{g}/\text{m}^3$ ).

### Surface Wipe Sampling.

Table 2 summarizes the concentrations of removable BPA and BPS from work surfaces and from parts that were printed with PESU or PC polymers. For PESU polymer, levels of BPA surface contamination were higher at the machinist's desk and the milling machines (26–200 ng/100 cm<sup>2</sup>) in the machining bay compared with surfaces of LFAM-1 (8–45 ng/100 cm<sup>2</sup>). The one exception was for wipe samples collected inside of LFAM-1 on the wall above the bucket used to collect purged waste polymer (preprint, <6–266 ng/100 cm<sup>2</sup>; postprint, 127–567 ng/100 cm<sup>2</sup>). The waste bucket is only emptied intermittently, so this higher BPA level on the wall near the waste bucket likely reflects contamination accrued from multiple print jobs over time. For PESU polymer, there was no evidence of accumulation of BPA on surfaces during a print job. Wipe samples for BPS revealed a similar pattern of higher levels at the machinist's desk and the milling machines (0.3–2.7 ng/100 cm<sup>2</sup>) in the machining bay compared with surfaces of LFAM-1 (<0.22–0.92 ng/100 cm<sup>2</sup>). BPA and BPS were present on surfaces of parts before and after they were machined.

There was evidence of BPA accumulation during a PC polymer print job on the machine door (preprint, 161 ng/100 cm<sup>2</sup>; postprint, 267 ng/100 cm<sup>2</sup>) and wall (preprint, 14 ng/100 cm<sup>2</sup>; postprint, 38 ng/100 cm<sup>2</sup>) surfaces inside the LFAM-1 enclosure. Additionally, there was approximately 50 ng/100 cm<sup>2</sup> removable BPA surface contamination on printed PC parts before and after they were machined. BPS levels on most wipe samples collected when PC polymer was in use were below the analytical limit of detection, though measurable levels were observed on commonly touched surfaces such as a computer keyboard (approximately 0.4 ng/100 cm<sup>2</sup>). BPS contamination on printed parts ranged from <0.28 to 0.93 ng/100 cm<sup>2</sup>.

## DISCUSSION

Herein, we reported the physical and chemical composition of particles and gases released during LFAM of ABS and PC as well as the high-melt-temperature polymers Ultem, PPS, PSU, and PESU. In general, most area air sample concentrations were well below occupational exposure limits (OELs). For example, the maximum concentration of Zn was 0.1 mg/m<sup>3</sup> (Ultem), which was a factor of 50 lower than the NIOSH recommended exposure limit (REL) of 5 mg/m<sup>3</sup> for zinc as zinc oxide.<sup>42</sup> Outside of the LFAM enclosures, levels of airborne BPA did not exceed 2 µg/m<sup>3</sup>; the German MAK for BPA is 5 mg/m<sup>3</sup> (there is no NIOSH REL for BPA).<sup>43</sup> The highest measured concentration of caprolactam was 22 µg/m<sup>3</sup>, well below the NIOSH REL of 1 mg/m<sup>3</sup>.<sup>42</sup> Only formaldehyde was measured at a concentration that approached its OEL. Airborne concentrations ranged from 12.8 µg/m<sup>3</sup> (ABS) to 18.8 µg/m<sup>3</sup> (Ultem); NIOSH considers this substance to be a potential occupational carcinogen with an REL of 19.7 µg/m<sup>3</sup>.<sup>42</sup> Some caution is warranted in the interpretation of these comparisons because the results are from area air sampling; future personal air sampling is needed to determine actual worker exposures.

In the current study, for all polymers, aerosol particle morphologies generally fell into three regimes: (1) diffuse clusters (Figure S1), (2) fibers from infill material, and (3) compact particles. Figure 1 illustrated the observed fiber and compact particle morphology regimes using example images collected from all of the polymers during printing. Fiber

Author Manuscript

Author Manuscript

Author Manuscript

Author Manuscript

morphologies (Figure 1a,b) included large fibers (approximately 4  $\mu\text{m}$  diameter by 30  $\mu\text{m}$  long) with low probability of inhalation and small respirable fragments. Compact particle morphologies (Figure 1c–f) included submicron- and micron-scale respirable particles; some compact particles had a smooth spherical shape whereas others had an irregular shape. Several studies of material extrusion-type printer emissions have also reported cluster and compact particle morphologies and noted variation in size, shape, and surface topography.<sup>15,19,20,44–46</sup> A number of factors may contribute to morphology of aerosolized particles released during printing, including print parameters (temperature, extrusion rate, etc.) and polymer properties.

Airborne particles contained several metals, some of which are respiratory irritants (aluminum, arsenic, copper, tin, and zinc), asthmagens (chromium, manganese, nickel, and vanadium), and possible occupational carcinogens (arsenic, nickel, and vanadium)<sup>42</sup> at concentrations generally less than 100  $\mu\text{g}/\text{m}^3$ . Other investigators have reported the presence of these metals in aerosol released from material extrusion type printers as well as iron, silicon, cobalt, molybdenum, lead, and titanium.<sup>12–15,17,20,45</sup> In the current study, the exact source of metals in emitted aerosol particles is unknown. From Table 1, none of the polymer structures contained metals. A prior study of emissions from polymer filaments extruded in desktop-scale FFF 3-D printers observed the presence of several metals that were attributed by those authors as pigments to add color to polymers.<sup>14</sup> Most polymers were black. Carbon black is the predominant pigment used to impart a black color in polymers, though metal-based additives or catalyst residues are often present in black polymers.<sup>47,48</sup> One polymer (ABS with GF) was white. Titanium dioxide is the most common pigment used to color polymers white.<sup>47,48</sup> Hence, it is possible that the observed metals in air samples were from the pigment used to color unmodified polymer black or white during manufacture. Alternatively, these metals could be additives or manufacturing residues, though elemental analysis was not performed on the bulk feedstock to verify this supposition.

BPA monomer is used in the manufacture of PC and can affect the male reproductive system and likely the female reproductive system.<sup>28,49,50</sup> Previously, Gu et al.<sup>8</sup> reported that BPA, possibly present as a plasticizer, was emitted during extrusion of ABS; however, no samples for BPA were collected during the ABS print jobs in this study because it was an unrecognized hazard by us at the time of our data collection. BPS is a replacement chemical for BPA and is used in the manufacture of PSU and PESU but may cause similar adverse endocrine disruptive health effects.<sup>36,51</sup> Both BPA and BPS may accumulate in fetuses via maternal transfer, and BPA is known to accumulate in several tissues in adults.<sup>52,53</sup> BPA was quantified in particulate air samples collected during extrusion of PC polymer, and both BPA and BPS were quantified in air samples collected during extrusion of PESU polymers. To our knowledge, BPA has not previously been assessed in field studies of AM process emissions, and BPS has not been reported in any AM emissions study. The average airborne BPA levels observed during extrusion of PC and PESU polymers (0.4–21.3  $\mu\text{g}/\text{m}^3$ ) were lower than those reported in workplace air of facilities that produced BPA-containing casting waxes (48  $\mu\text{g}/\text{m}^3$ ) but similar or higher than those reported for phenolic resin manufacturing (0.62–0.85  $\mu\text{g}/\text{m}^3$ ) and in a PC polymer injection molding factory (0.008–0.028  $\mu\text{g}/\text{m}^3$ ).<sup>41,54</sup> Both BPA and BPS were present on surface wipe samples, which indicated potential for dermal exposure, a known exposure pathway, for these substances.<sup>41,55</sup>

In this facility, levels of BPA on surfaces in the machining area and LFAM-1 (<8–587 ng/100 cm<sup>2</sup>) were much lower than reported for break rooms (6.5 µg/100 cm<sup>2</sup>) and production areas (140 µg/100 cm<sup>2</sup>) in wax casting and phenolic resin production workplaces.<sup>41</sup> It was observed that levels of BPA and BPS were generally higher on surfaces in the machining bay compared with surfaces on LFAM-1. The machining bay is an open floor plan, with the operator's desk positioned approximately equidistant between milling machines A and B. Due to the size of the milling machines, neither is fully enclosed. Rather, movable acrylic wall partitions are positioned around the milling machines to create a safety barrier between the operator and moving arm of the machine. The higher levels of BPA and BPS in the machining bay may reflect unhindered spread of aerosol from the milling machines over time and/or deposition of vapor-phase BPA and BPS that was evaporated by heat generated at the interface of the milling tool bit and part. For LFAM-1, wipe samples were collected in the same locations before and after a print job. Results in Table 2 indicated that some pairs of wipe samples were higher after a print job compared with before the print job, which indicated an accumulation of surface contamination. For other pairs of surface wipe samples, the postprint level of BPA or BPS was lower than the preprint level. It is unclear if a lower observed postprint level represented residual BPA or BPS from inefficient removal of contaminants during collection of the preprint sample or complete removal by the preprint sample and reaccumulation during printing. Again, BPA and BPS on surfaces may be from dispersion of aerosol or deposition of vapor-phase compounds. Finally, it is important to note that BPA and BPS were present on surfaces of parts after they were printed and after they were machined, which indicated the potential for dermal exposure extended beyond printing to postprint processing tasks such as machining and handling as well as the end users of these parts. Collectively, these air and surface wipe results for BPA and BPS revealed that a previously unrecognized exposure risk may be occurring in AM facilities that extrude or machine PC and PESU polymers. Given their endocrine disrupting potential, precautions should be considered to reduce airborne and surface contamination of BPA and BPS to mitigate inhalation and dermal exposure.

Numerous organic and inorganic gases were quantified by air sampling, including respiratory irritants (benzene, formaldehyde, phenol, SO<sub>2</sub>, toluene, and xylenes),<sup>42</sup> possible or known asthmagens (caprolactam, methyl methacrylate, 4-oxopentanal, and styrene),<sup>21,42,56–58</sup> and substances identified by NIOSH as possible occupational carcinogens (benzene and aldehydes).<sup>42</sup> The relatively low levels of these substances are somewhat surprising given that up to hundreds of kilograms of polymer were extruded during a print job. However, each polymer contained 20–50% by weight of CF or GF additive, so the mass of plastic that underwent thermal breakdown was less than the total mass of extruded polymer.

## Supplementary Material

Refer to Web version on PubMed Central for supplementary material.

## ACKNOWLEDGMENTS

The authors thank Dr. R. LeBouf, D. Burns, and A. Ranpara at NIOSH for analysis of the canister samples and Dr. S. Linde (North West University) and Dr. W. Chisholm (NIOSH) for critical review of this manuscript prior

to submission to the journal. We also thank the company where these measurements were performed for access to their facility. The findings and conclusions in this report are those of the authors and do not necessarily represent the official position of the National Institute for Occupational Safety and Health, Centers for Disease Control and Prevention. This work was supported by NIOSH intramural research funds. The South African Department of Science and Innovation through the Competitive Programme in Additive Manufacturing funded the research visit of J.L.d.P. and S.d.P.

## REFERENCES

- (1). Stefaniak A; Bowers L; Martin JS; Hammond D; Ham J; Wells J; Fortner A; Knepp A; du Preez S; Pretty JR; Roberts JL; du Plessis J; Duling MG; Virji MA Large-Format Additive Manufacturing and Machining Using High-Melt-Temperature Polymers. Part I: Real-Time Particulate and Gas-Phase Emissions. *ACS Chem. Health Safe* 2021, in press. DOI: 10.1021/acs.chas.0c00128
- (2). Azimi P; Zhao D; Pouzet C; Crain NE; Stephens B Emissions of ultrafine particles and volatile organic compounds from commercially available desktop three-dimensional printers with multiple filaments. *Environ. Sci. Technol* 2016, 50, 1260–8. [PubMed: 26741485]
- (3). Chan FL; Hon CY; Tarlo SM; Rajaram N; House R Emissions and health risks from the use of 3D printers in an occupational setting. *J. Toxicol. Environ. Health, Part A* 2020, 83, 279–87.
- (4). Davis AY; Zhang Q; Wong JPS; Weber RJ; Black MS Characterization of volatile organic compound emissions from consumer level material extrusion 3D printers. *Build Environ* 2019, 160, No. 106209.
- (5). Ding S; Ng BF; Shang X; Liu H; Lu X; Wan MP The characteristics and formation mechanisms of emissions from thermal decomposition of 3D printer polymer filaments. *Sci. Total Environ* 2019, 692, 984–94. [PubMed: 31540002]
- (6). du Preez S; Johnson AR; LeBouf RF; Linde SJL; Stefaniak AB; Du Plessis J Exposures during industrial 3-D printing and post-processing tasks. *Rapid Proto J* 2018, 24, 865–71.
- (7). Floyd EL; Wang J; Regens JL Fume emissions from a low-cost 3-D printer with various filaments. *J. Occup. Environ. Hyg* 2017, 14, 523–33. [PubMed: 28406364]
- (8). Gu J; Wensing M; Uhde E; Salthammer T Characterization of particulate and gaseous pollutants emitted during operation of a desktop 3D printer. *Environ. Int* 2019, 123, 476–85. [PubMed: 30622073]
- (9). Kim Y; Yoon C; Ham S; Park J; Kim S; Kwon O; Tsai PJ Emissions of nanoparticles and gaseous material from 3D printer operation. *Environ. Sci. Technol* 2015, 49, 12044–53. [PubMed: 26402038]
- (10). Mendes L; Kangas A; Kukko K; Mølgaard B; Säämänen A; Kanerva T; Flores Ituarte I; Huhtiniemi M; Stockmann-Juvala H; Partanen J; Hämeri K; Eleftheriadis K; Viitanen AK Characterization of emissions from a desktop 3D printer. *J. Ind. Ecol* 2017, 21, S94–S106.
- (11). Potter PM; Al-Abed SR; Lay D; Lomnicki SM Voc emissions and formation mechanisms from carbon nanotube composites during 3D printing. *Environ. Sci. Technol* 2019, 53, 4364–70. [PubMed: 30875473]
- (12). Stefaniak AB; Johnson AR; du Preez S; Hammond DR; Wells JR; Ham JE; LeBouf RF; Martin SBJ; Duling MG; Bowers LN; Knepp AK; de Beer DJ; JL dP. Insights into emissions and exposures from use of industrial-scale additive manufacturing machines. *Saf. Health Work.* 2019, 10, 229–236. [PubMed: 31297287]
- (13). Stefaniak AB; Johnson AR; du Preez S; Hammond DR; Wells JR; Ham JE; LeBouf RF; Menchaca KW; Martin SBJ; Duling MG; Bowers LN; Knepp AK; Su FC; de Beer DJ; JL dP. Evaluation of emissions and exposures at workplaces using desktop 3-dimensional printers. *J. Chem. Health Saf* 2019, 26, 19–30. [PubMed: 31798757]
- (14). Stefaniak AB; LeBouf RF; Yi J; Ham JE; Nurkewicz TR; Schwegler-Berry DE; Chen BT; Wells JR; Duling MG; Lawrence RB; Martin SB Jr; Johnson AR; Virji MA Characterization of chemical contaminants generated by a desktop fused deposition modeling 3-dimensional printer. *J. Occup. Environ. Hyg* 2017, 14, 540–50. [PubMed: 28440728]
- (15). Steinle P Characterization of emissions from a desktop 3D printer and indoor air measurements in office settings. *J. Occup. Environ. Hyg* 2016, 13, 121–32. [PubMed: 26550911]

(16). Väistönen AJK; Hyttinen M; Ylönen S; Alonen L Occupational exposure to gaseous and particulate contaminants originating from additive manufacturing of liquid, powdered and filament plastic materials and related post-processes. *J. Occup. Environ. Hyg* 2019, 16, 258–71. [PubMed: 30540539]

(17). Vance ME; Pegues V; Van Montfrans S; Leng W; Marr LC Aerosol emissions from fuse-deposition modeling 3D printers in a chamber and in real indoor environments. *Environ. Sci. Technol* 2017, 51, 9516–23. [PubMed: 28789516]

(18). Wojtyła S; Klama P; piewak K; Baran T 3D printer as a potential source of indoor air pollution. *Int. J. Environ. Sci. Technol* 2020, 17, 207–18.

(19). Youn JS; Seo JW; Han S; Jeon KJ Characteristics of nanoparticle formation and hazardous air pollutants emitted by 3D printer operations: From emission to inhalation. *RSC Adv* 2019, 9, 19606–12. [PubMed: 35519372]

(20). Zontek TL; Ogle BR; Jankovic JT; Hollenbeck SM An exposure assessment of desktop 3D printing. *J. Chem. Health Saf* 2017, 24, 15–25.

(21). Chan FL; House R; Kudla I; Lipszyc JC; Rajaram N; Tarlo SM Health survey of employees regularly using 3D printers. *Occup Med. (Lond)* 2018, 68, 211–14. [PubMed: 29538712]

(22). House R; Rajaram N; Tarlo SM Case report of asthma associated with 3D printing. *Occup Med. (Lond)* 2017, 67, 652–54. [PubMed: 29016991]

(23). Stefaniak AB; LeBouf RF; Duling MG; Yi J; Abukabda AB; McBride CR; Nurkiewicz TR Inhalation exposure to three-dimensional printer emissions stimulates acute hypertension and microvascular dysfunction. *Toxicol. Appl. Pharmacol* 2017, 335, 1–5. [PubMed: 28942003]

(24). Zhang Q; Pardo M; Rudich Y; Kaplan-Ashiri I; Wong JPS; Davis AY; Black MS; Weber RJ Chemical composition and toxicity of particles emitted from a consumer-level 3D printer using various materials. *Environ. Sci. Technol* 2019, 53, 12054–61. [PubMed: 31513393]

(25). Farcas MT; Stefaniak AB; Knepp AK; Bowers L; Mandler WK; Kashon M; Jackson SR; Stueckle TA; Sisler JD; Friend SA; Qi C; Hammond DR; Thomas TA; Matheson J; Castranova V; Qian Y Acrylonitrile butadiene styrene (ABS) and polycarbonate (PC) filaments three-dimensional (3-D) printer emissions-induced cell toxicity. *Toxicol. Lett* 2019, 317, 1–12. [PubMed: 31562913]

(26). Wojtyła S; Klama P; Baran T Is 3D printing safe? Analysis of the thermal treatment of thermoplastics: ABS, PLA, PET, and nylon. *J. Occup. Environ. Hyg* 2017, 14, D80–D85. [PubMed: 28165927]

(27). He Z; Li G; Chen J; Huang Y; An T; Zhang C Pollution characteristics and health risk assessment of volatile organic compounds emitted from different plastic solid waste recycling workshops. *Environ. Int* 2015, 77, 85–94. [PubMed: 25667057]

(28). Šala M; Kitahara Y; Takahashi S; Fujii T Effect of atmosphere and catalyst on reducing bisphenol A (BPA) emission during thermal degradation of polycarbonate. *Chemosphere* 2010, 78, 42–45. [PubMed: 19900691]

(29). Koo JH; Venumbaka S; Cassidy PE; Fitch JW; Grand AF; Bundick J Flammability studies of thermally resistant polymers using cone calorimetry. *Fire Mater* 2000, 24, 209–18.

(30). Ehlers GFL; Fisch KR; Powell WR Thermal degradation of polymers with phenylene units in the chain. II. Sulfur-containing polyarylenes. *J. Polym. Sci. Part A-1: Polym. Chem* 1969, 7, 2955–67.

(31). Budgell DR; Day M; Cooney JD Thermal degradation of poly(phenylene sulfide) as monitored by pyrolysis-GC/MS. *Polym. Degrad. Stab* 1994, 43, 109–15.

(32). Almén P; Ericsson I Studies of the thermal degradation of polysulfones by filament-pulse pyrolysis-gas chromatography. *Polym. Degrad. Stab* 1995, 50, 223–28.

(33). Perng LH Thermal degradation mechanism of poly(arylene sulfone)s by stepwise py-GC/MS. *J. Polym. Sci. Part A: Polym. Chem* 2000, 38, 583–93.

(34). Perng LH Comparison of thermal degradation characteristics of poly(arylene sulfone)s using thermogravimetric analysis/mass spectrometry. *J. Appl. Polym. Sci* 2001, 81, 2387–89.

(35). Shabaev AS; Zhansitov AA; Kurdanova ZI; Khashirova SY; Mikitaev AK New method of investigation of polysulfone thermal destruction. *Polym. Sci. Ser. B* 2017, 59, 216–24.

(36). Gorence GJ; Pulcastro HC; Lawson CA; Gerona RR; Friesen M; Horan TS; Gieske MC; Sartain CV; Hunt PA Chemical contaminants from plastics in the animal environment. *J. Am. Assoc. Lab. Anim. Sci* 2019, 58, 190–96. [PubMed: 30646968]

(37). Horan TS; Pulcastro H; Lawson C; Gerona R; Martin S; Gieske MC; Sartain CV; Hunt PA Replacement bisphenols adversely affect mouse gametogenesis with consequences for subsequent generations. *Curr. Biol* 2018, 28, 2948–2954.e3. [PubMed: 30220498]

(38). Ham JE; Jackson SR; Harrison JC; Wells JR Gas-phase reaction products and yields of terpinolene with ozone and nitric oxide using a new derivatization agent. *Atmos. Environ* 2015, 122, 513–20.

(39). Jackson SR; Ham JE; Harrison JC; Wells JR Identification and quantification of carbonyl-containing  $\alpha$ -pinene ozonolysis products using o-tert-butylhydroxylamine hydrochloride. *J. Atmos Chem* 2016, 74 (3), 325–338. [PubMed: 28701805]

(40). Wells JR; Ham JE A new agent for derivatizing carbonyl species used to investigate limonene ozonolysis. *Atmos. Environ* 2014, 99, 519–26.

(41). Hines CJ; Jackson MV; Christianson AL; Clark JC; Arnold JE; Pretty JR; Deddens JA Air, hand wipe, and surface wipe sampling for bisphenol A (BPA) among workers in industries that manufacture and use BPA in the United States. *J. Occup. Environ. Hyg* 2017, 14, 882–97. [PubMed: 28650732]

(42). NIOSH. *Pocket Guide to Chemical Hazards*, 2018. <http://www.cdc.gov/niosh/npg/default.html> (accessed December 29, 2020).

(43). Hartwig A, Ed. List of MAK and BAT values 2015; Wiley-VCH: Bonn, Germany, 2015.

(44). Katz EF; Goetz JD; Wang C; Hart JL; Terranova B; Taheri ML; Waring MS; DeCarlo PF Chemical and physical characterization of 3D printer aerosol emissions with and without a filter attachment. *Environ. Sci. Technol* 2020, 54, 947–54. [PubMed: 31834782]

(45). Yi J; Duling MG; Bowers LN; Knepp AK; LeBouf RF; Nurkiewicz TR; Ranpara A; Luxton T; Martin SB Jr.; Burns DA; Peloquin DM; Baumann EJ; Virji MA; Stefaniak AB Particle and organic vapor emissions from children's 3-D pen and 3-D printer toys. *Inhalation Toxicol* 2019, 31, 432–45.

(46). Farcas MT; McKinney W; Qi C; Mandler KW; Battelli L; Friend SA; Stefaniak AB; Jackson M; Orandle M; Winn A; Kashon M; LeBouf RF; Russ KA; Hammond DR; Burns D; Ranpara A; Thomas TA; Matheson J; Qian Y Pulmonary and systemic toxicity in rats following inhalation exposure of 3-D printer emissions from acrylonitrile butadiene styrene (ABS) filament. *Inhalation Toxicol* 2020, 32, 403–18.

(47). Amba R In *Effect of pigments compounding on product performance*. SPE ANTEC Proceedings, 2015; Vol. 1, pp 1158–1622.

(48). Turner A Black plastics: Linear and circular economies, hazardous additives and marine pollution. *Environ. Int* 2018, 117, 308–18. [PubMed: 29778831]

(49). Richter CA; Birnbaum LS; Farabollini F; Newbold RR; Rubin BS; Talsness CE; Vandenberg JG; Walser-Kuntz DR; vom Saal FS In vivo effects of bisphenol A in laboratory rodent studies. *Reprod. Toxicol* 2007, 24, 199–224. [PubMed: 17683900]

(50). Huang J; He C; Li X; Pan G; Tong H Theoretical studies on thermal degradation reaction mechanism of model compound of bisphenol A polycarbonate. *Waste Manage* 2018, 71, 181–91.

(51). Grandin FC; Lacroix MZ; Gayrard V; Gauderat G; Mila H; Toutain PL; Picard-Hagen N Bisphenol S instead of bisphenol A: Toxicokinetic investigations in the ovine materno-feto-placental unit. *Environ. Int* 2018, 120, 584–92. [PubMed: 30212803]

(52). Cimmino I; Fiory F; Perruolo G; Miele C; Beguinot F; Formisano P; Oriente F Potential mechanisms of bisphenol A (BPA) contributing to human disease. *Int. J. Mol. Sci* 2020, 21, No. 5761.

(53). Gingrich J; Filipovic D; Conolly R; Bhattacharya S; Veiga-Lopez A Pregnancy-specific physiologically-based toxicokinetic models for bisphenol A and bisphenol A. *Environ. Int* 2021, 147, No. 106301.

(54). Kouidhi W; Thannimalay L; Soon CS; Mohd MA Occupational exposure to bisphenol A (BPA) in a plastic injection molding factory in Malaysia. *Int. J. Occup. Med. Environ. Health* 2017, 30, 743–750. [PubMed: 28584331]

(55). Champmartin C; Marquet F; Chedik L; Decret MJ; Aubertin M; Ferrari E; Grandclaude MC; Cosnier F Human in vitro percutaneous absorption of bisphenol S and bisphenol A: A comparative study. *Chemosphere* 2020, 252, 126525. [PubMed: 32220717]

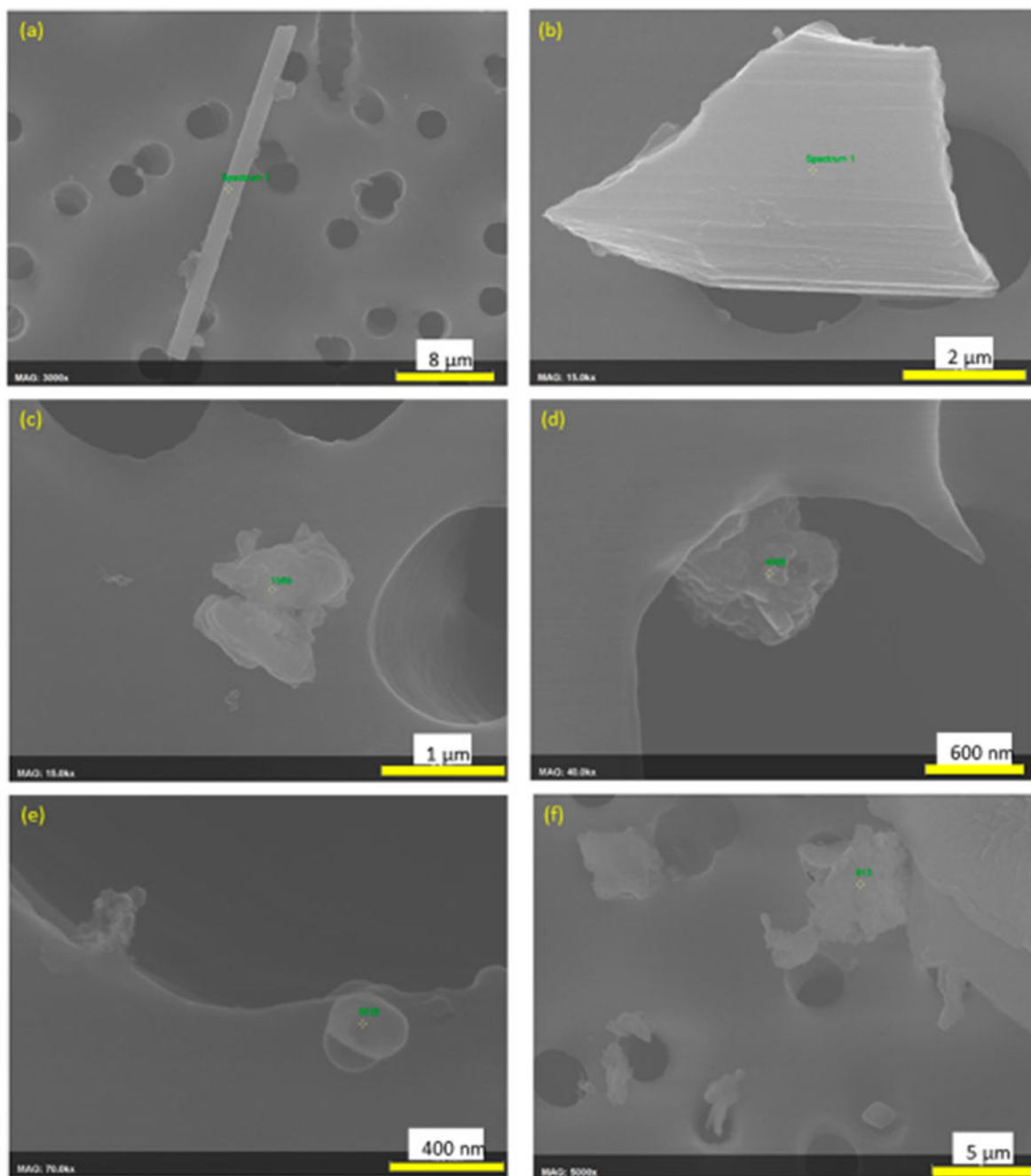
(56). Moscato G; Biscaldi G; Cottica D; Pugliese F; Candura S; Candura F Occupational asthma due to styrene: Two case reports. *J. Occup Med* 1987, 29, 957–960. [PubMed: 3430203]

(57). Van Kampen V; Merget R; Baur X Occupational airway sensitizers: An overview on the respective literature. *Am. J. Ind. Med* 2000, 38, 164–218. [PubMed: 10893510]

(58). Anderson SE; Franko J; Jackson LG; Wells JR; Ham JE ; Meade BJ Irritancy and allergic responses induced by exposure to the indoor air chemical 4-oxopentanal. *Toxicol. Sci* 2012, 127, 371–81. [PubMed: 22403157]

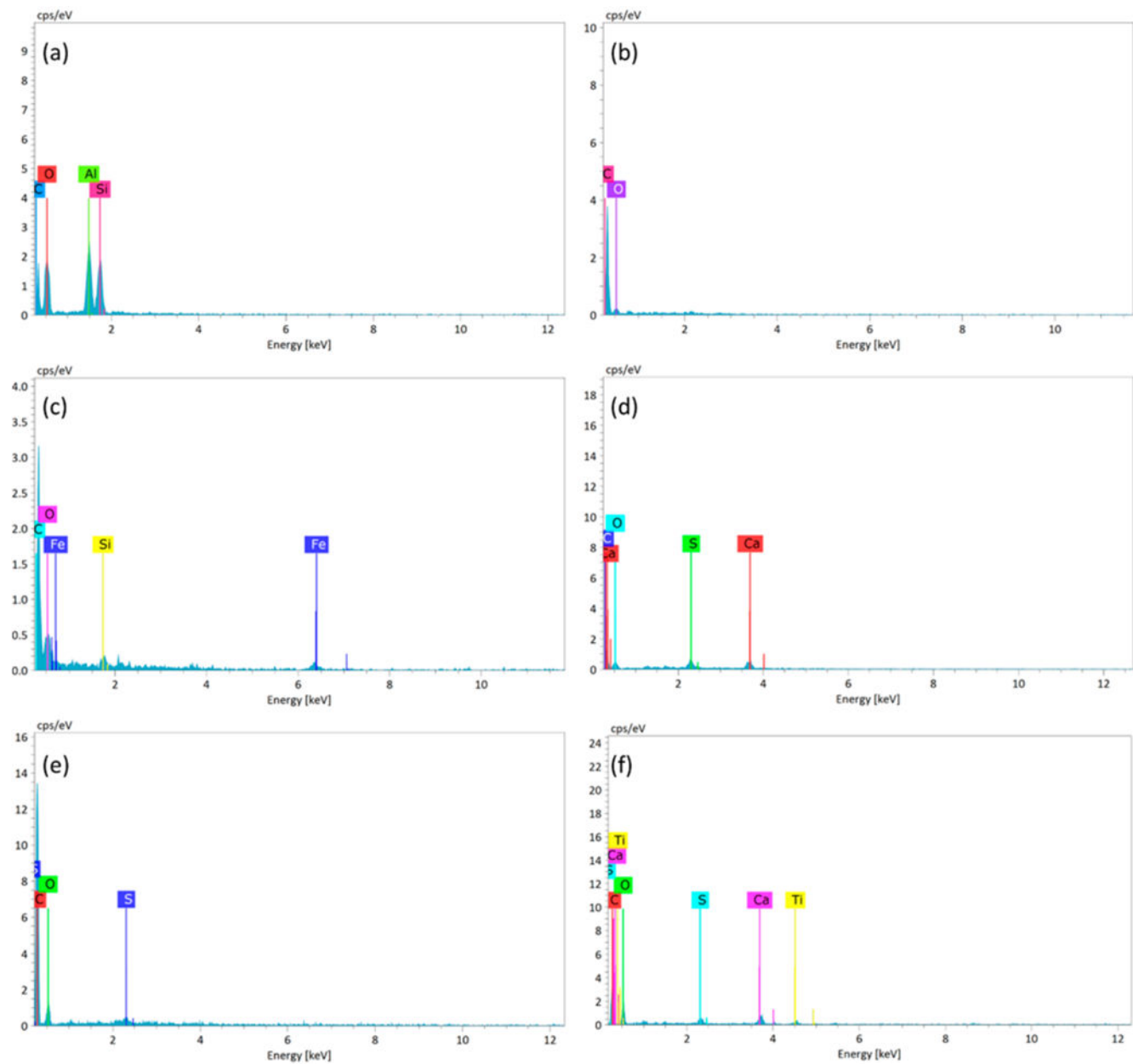
**SUMMARY**

Results presented herein indicated that extrusion of ABS and PC as well as high-melt-temperature PSU, PPS, Ultem, and PESU released particles and gases with characteristics that varied by polymer type. Notably, we quantified BPA and BPS in air and surface wipe samples, which indicated that PC and PESU polymers were sources for potential inhalation and dermal exposure to these endocrine disrupting chemicals. Additionally, low levels of respiratory irritants, asthmagens, and possible occupational carcinogens were quantified in workplace air. The release of submicrometer particles (Part I companion paper) coupled with characteristics of particles and gases identified in this report support the need for polymer-specific exposure and risk assessments to inform decision making on engineering controls.

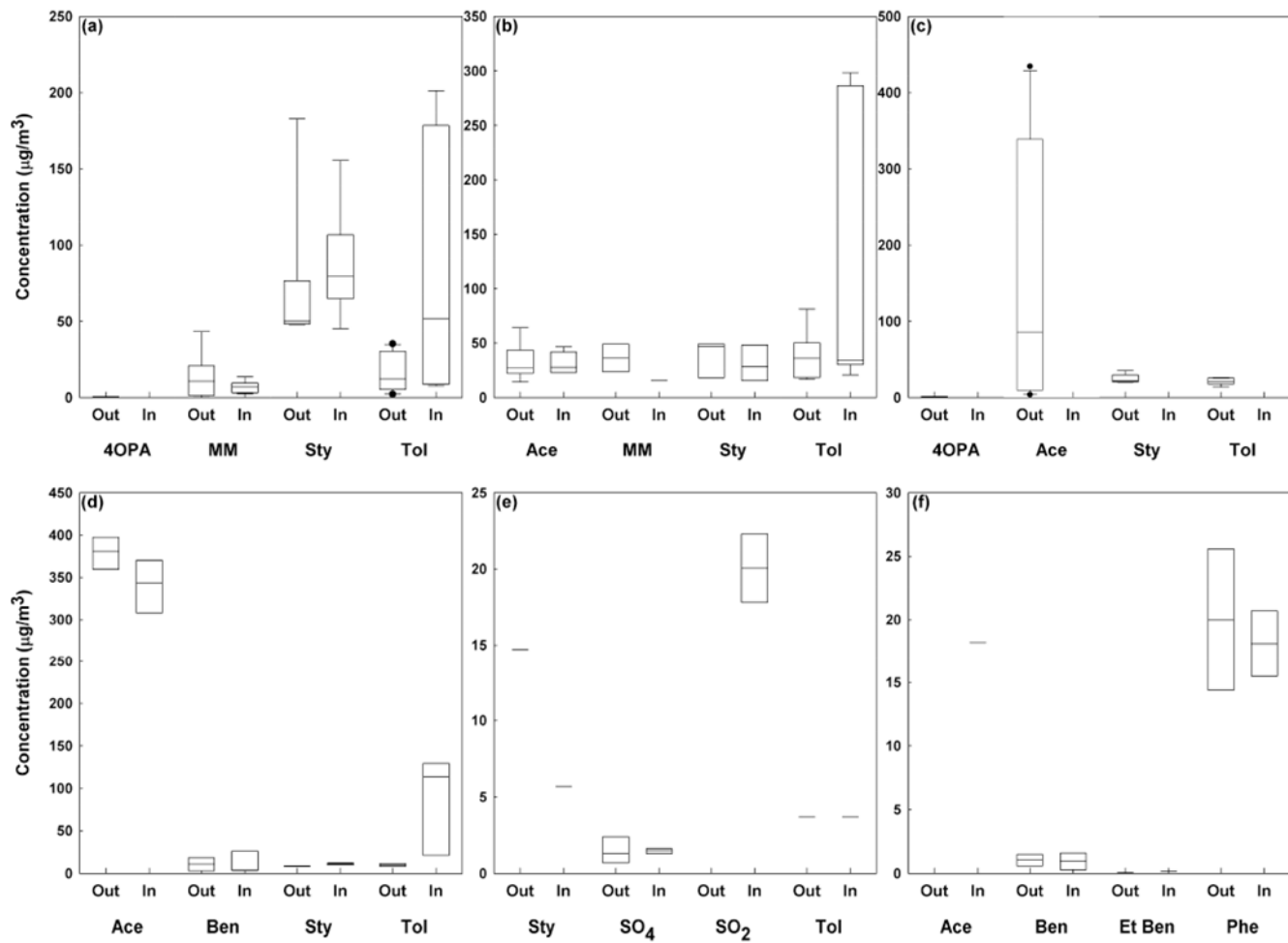


**Figure 1.**

Morphology of aerosol particles released during polymer extrusion: (a) fiber-shaped particle (ABS), (b) micron-scale fiber fragment (PC), (c) micron-scale particle (Ultem), (d) submicron-scale particle (PPS), (e) nanoscale particle (PSU), and (f) micron-scale particle (PESU). Note that scale bars differ among images.

**Figure 2.**

Elemental spectra of particles (presented in Figure 1): (a) fiber-shaped particle composed of carbon, oxygen, aluminum, and silicon (ABS); (b) micron-scale fiber fragment composed of carbon and oxygen (PC); (c) micron-scale particle composed of carbon, oxygen, iron, and silicon (Ultem); (d) submicron-scale particle composed of carbon, oxygen, and sulfur (PPS); (e) nanoscale particle composed of carbon, oxygen, and sulfur (PSU); and (f) micron-scale particle that contained calcium, sulfur, and titanium (PESU).

**Figure 3.**

Box plots of time-integrated sampling results for select substances released during extrusion of (a) ABS, (b) PC, (c) Ultem, (d) PPS, (e) PSU, and (f) PESU polymers. Out = outside sampling location. In = inside sampling location. Ace = acetone. Ben = benzene. Et Ben = ethylbenzene. MM = methyl methacrylate. 4OPA = 4-oxopentanal. Phe = phenol.  $\text{SO}_4$  = sulfate.  $\text{SO}_2$  = sulfur dioxide. Sty = styrene. Tol = toluene.

Author Manuscript

Author Manuscript

Author Manuscript

Author Manuscript

Table 1.

Polymer Type and Extrusion Conditions during Large Format Additive Manufacturing and Reported Emissions and Thermal Breakdown Products from the Available Literature

Polymer	Chemical name	Chemical structure	Nozzle (°C)	Platform (°C)	Emissions/breakdown products <sup>a</sup>
ABS	Acrylonitrile butadiene styrene		240 – 270	20 – 110	• Acetaldehyde • Particles • Metals <sup>b</sup> • Acetone • Benzene • BPA • $\alpha$ -Pinene • Styrene • 1-Butanol • Caprolactam • Formalddehyde • Toluene
PC	Polycarbonate		265 – 305	100 – 120	• Toluene • Xylenes • Particles • Metals <sup>b</sup> • Caprolactam • Ethylbenzene • Heptane • Pentane • BPA • Styrene • CO <sub>2</sub>
Ultem®	Polyetherimide		385	20 – 120	• Acetone • Particles • Metals <sup>b</sup> • CO • CO <sub>2</sub>
PPS	Polyphenylene sulfide		360	125	• Benzene • Benzene thiol • H <sub>2</sub> S • SO <sub>2</sub> • CO • CO <sub>2</sub> • CS <sub>2</sub>
PSU	Polysulfone		350	148	• Benzene • Dibenzofuran • Ethylbenzene • Styrene • m,p-Xylene
PESU	Polyethersulfone		438	148	• Benzene • Chlorobenzene • Dibenzofuran • Phenol • SO <sub>2</sub>

<sup>a</sup> ABS: desktop-scale material extrusion 3-D printer emissions; <sup>b</sup> PC: desktop-scale material extrusion 3-D printer emissions; <sup>2,7–10,13–15,18</sup> thermogravimetric analysis; <sup>26</sup> PC: desktop-scale material extrusion 3-D printer emissions; <sup>2,8</sup> plastics recycling; <sup>27</sup> heating in air; <sup>28</sup> Ultim: industrial-scale material extrusion printer emission; <sup>12</sup> pyrolysis; <sup>29</sup> PPS: heating between 20 and 450 °C; <sup>30</sup> pyrolysis; <sup>31</sup> PSU: heating between 20 and 450 °C; <sup>32,35</sup> leaching; <sup>36,37</sup> PESU: pyrolysis. <sup>32–34</sup>

<sup>b</sup>The chemical structures of ABS, PC, and Ultim do not contain metals, which suggests the presence of additives or impure ingredients in polymers.

**Table 2.**

Blank-Corrected Concentrations of BPA and BPS on Surfaces

sample location	BPA (ng/100 cm <sup>2</sup> )	BPS (ng/100 cm <sup>2</sup> )
PESU Polymer, November 14, 2018: Machinist's Desk Area		
file cabinet drawer	104	1.9
desktop	189	2.5
computer keyboard	26	0.6
PESU Polymer, November 14, 2018: Milling Machines		
machine A, wall panel (inside)	148	0.3
machine B, control panel	200	0.7
PESU Polymer, November 14, 2018: Printed Parts		
premachined scrap cut from part	16	0.4
postmachined part	<8	1.9
PESU Polymer, November 13, 2019: LFAM-1		
computer keyboard (preprint)	45	0.41
computer keyboard (postprint)	29	<0.22
acrylic door handles (preprint)	18	0.88
acrylic door handles (postprint)	16	0.49
wall, inside enclosure (preprint)	9	<0.22
wall, inside enclosure (postprint)	8	<0.22
wall, by waste bucket inside enclosure (preprint)	266	0.34
wall, by waste bucket inside enclosure (postprint)	127	<0.22
PESU Polymer, November 13, 2019: Printed Parts		
immediately after printing (November 13)	<6	<0.22
day after printing (November 14)	<6	<0.22
postmachined part (printed on November 12)	11	<0.22
PESU Polymer, November 14, 2019: LFAM-1		
computer keyboard (preprint)	20	0.50
computer keyboard (postprint)	13	<0.22
acrylic door handles (preprint)	19	0.92
acrylic door handles (postprint)	20	0.54
wall, inside enclosure (preprint)	<6	<0.22
wall, by waste bucket inside enclosure (preprint)	587	<0.22
PC Polymer, November 15, 2018: LFAM-1		
computer keyboard (preprint)	22	0.36
computer keyboard (postprint)	15	0.38
acrylic door panel, outside enclosure (preprint)	22	<0.28
acrylic door panel, outside enclosure (postprint)	17	<0.28
acrylic door panel, inside enclosure (preprint)	161	2.5
acrylic door panel, inside enclosure (postprint)	267	1.3
wall, inside enclosure (preprint)	14	<0.28
wall, inside enclosure (postprint)	38	<0.28

sample location	BPA (ng/100 cm <sup>2</sup> )	BPS (ng/100 cm <sup>2</sup> )
print bed (postprint)	43	<0.28
PC Polymer, November 15, 2018: Printed Parts		
postmachined (printed on November 13)	53	0.43
premachined (printed on November 13)	55	<0.28